

A Study on the Corrosion Inhibition Performance of Various Starches for Q235A Steel

Di MA*, Shubai LI, Dongmei YU, Jie GONG, Jushi WENG, Zou CHEN, XingJian TAN

School of Chemistry & Environmental Engineering, Jiangsu University of Technology, Changzhou, China

<http://doi.org/10.5755/j02.ms.40070>

Received 6 January 2025; accepted 29 April 2025

Eight different varieties of starch were chosen to replace the corrosion inhibitors in order to assess the corrosion resistance and rate of deterioration of Q235A steel using an electrochemical test and the weightlessness method. The metallographic microscope was used to examine the corrosion product surface on the steel plate. The results of the weightless method show that the corrosion rate of 300 mg/L of starch was higher than the concentration of 500 mg/L. As the concentration of H₂SO₄ was 0.5 mol/L, the corrosion rate of 300 mg/L of cassava starch, mung bean starch, and wheat starch solution was higher than the others, which were 72.92 %, 72.89 %, and 72.02 %. The results of the electrochemical test show that the corrosion resistance of 300 mg/L pea starch and cassava starch solution were better in the condition of 0.5 mol/L H₂SO₄, whose self-corrosion currents were 34 $\mu\text{A}\cdot\text{cm}^{-2}$ and 26 $\mu\text{A}\cdot\text{cm}^{-2}$. Their solution resistance R_s were 1.739 $\Omega\cdot\text{cm}^{-2}$ and 1.801 $\Omega\cdot\text{cm}^{-2}$, respectively. In conclusion, the effect of 300 mg/L of tapioca starch and pea starch was better in 0.5 mol/L H₂SO₄ solution.

Keywords: weightlessness method, corrosion rate, corrosion resistance, starch.

1. INTRODUCTION

With the advent of the "green chemistry" concept in the new century, a profound transformation has occurred in the trajectory of world chemistry and the chemical industry. Consequently, the pursuit of eco-friendly corrosion inhibitors has emerged as a pivotal research avenue and a frontier in natural science [1–3].

Although starch has long been recognized as a natural organic polymer with applications in areas such as scale prevention and corrosion inhibition [3], in-depth and clear research on the specific distinctions and underlying mechanisms of its corrosion-inhibitory effects on metals is still lacking. The current understanding of the impact that various types of starches exert on metal corrosion inhibition remains murky. Further research and exploration are necessary to understand the effects and mechanisms of different starch types in metal corrosion inhibition.

This paper explores starch-based corrosion inhibitors, utilizing eight different starches as the foundation for our investigation: mung bean, potato, wheat, pea, tapioca, sweet potato, corn, and rice starch. Electrochemical experiments were used to systematically examine these starches, to identify the most effective concentration of each starch-based inhibitor in various acidic environments. Subsequently, the optimal concentration for each inhibitor under these conditions was determined, allowing for a comprehensive comparison of their corrosion inhibition effects. This analysis provides insights into the relative performance of these inhibitors in diverse acidic settings.

2. MATERIALS AND METHODS

This experiment utilized Q235A carbon structural steel, and its main chemical composition is listed in Table 1. The dimensions of the steel sheet samples used in the experiment were 20 mm × 100 mm × 1 mm.

Table 1. Main chemical composition of Q235A sample

Element	Mn	Si	P	S	C	Fe
$\omega, \%$	1.4	0.35	0.045	0.050	0.22	1.4

A sulfuric acid solution (H₂SO₄, 98 % purity) was diluted to a concentration of 0.5 mol/L using deionized water. A starch-based corrosion inhibitor was prepared by dissolving different starches (99.5 % purity) in deionized water under continuous stirring. The final concentration of the starch solution was adjusted to 300 mg/L and 500 mg/L.

The electrochemical properties of these samples were characterized by the CHI 660C electrochemical system given Tafel plots and electrochemical impedance spectroscopy (EIS). A conventional three-electrode electrochemical system was used, in which the samples as the working electrode, platinum foil was the counter electrode, and an Ag/AgCl electrode was the reference electrode. The electrochemical tests were conducted at room temperature ($25 \pm 1^\circ\text{C}$) under ambient atmospheric conditions. The Tafel plots (–0.2 to 0.6 V) and EIS spectra (0.1 Hz to 100 kHz) were collected in 0.1 M NaCl aqueous solution. The scan rate for CV was 0.1 Vs^{-1} and the oscillation potential for EIS was 10 mV. The microstructure of conversion coatings was characterized through Scanning Electron Microscopy (SEM) (SEM, Hitachi S-3400NII), and X-ray Photoelectron Spectroscopy (XPS, Thermo Fisher Scientific, ESCALAB 250Xi). X-ray diffraction (XRD) measurements were taken on a Rigaku D/max 2550VB/PC VB/PC Rigaku instrument. Cu $K\alpha$

* Corresponding author: D. Ma
E-mail: Madi@jsut.edu.cn

radiation ($\lambda = 1.5418 \text{ \AA}$) was obtained from a copper X-ray tube operated at 40 kV and 40 mA.

3. RESULTS AND DISCUSSION

The X-ray diffraction patterns (Fig. 1) of various plant starches can be summarized into three types: type A, type B, and type C. Most cereal starches, such as corn and rice, belong to type A, while most starches from roots and spherical rhizomes, such as potatoes, belong to type B, while most starches from roots and beans belong to type C.

The experimental wavelength is 1.5418 Å, the scanning voltage is 40 kV, the scanning current is 40 mA, the scanning step length is 0.05°, and the scanning range is 10 ~ 80°.

In Fig. 1 represent sweet potato starch, mung bean starch, potato starch, cassava starch, yam starch, pea starch, wheat starch, and corn starch, respectively. It can be seen from the figure that cassava starch, yam starch, wheat starch, and corn starch have strong diffraction peaks at 15°, 17°, 18°, and 23°, and there are double peaks, so they are A-type starch. Sweet potato starch has strong diffraction peaks at 17°, 22°, and 24°, so it is B-type starch. Mung bean starch, potato starch, and pea starch have both single peaks of A-type crystals and characteristic peaks of B-type crystals, so they are C-type starch [4].

The AC impedance spectra of starches at 300 and 500 mg/L in a 0.5 mol/L H₂SO₄ media are shown in Fig. 2. According to Fig. 2 a, the curves of sweet potato starch (HS), corn starch (YM), and tapioca starch (MS) have a significant capacitive arc under the condition of 300 mg/L concentration, indicating a robust corrosion resistance. Pea, wheat, and maize starch make up the bigger tolerance arc of the curve for 500 mg/L concentration, as shown in Fig. 2 b, and all three have high corrosion resistance. In conclusion, 100 mg/L of sweet potato starch (HS), corn starch (YM), and tapioca exhibit greater equivalent capacitive resistance arcs and stronger corrosion inhibition effects under the condition of 0.5 mol/L H₂SO₄.

The corrosion resistance parameters derived from the AC impedance spectra, as depicted in Fig. 2, are summarized in Table 2 and Table 3. To further address the distinct impedance spectra observed with varying starch types, an equivalent circuit was used to fit the experimental data from the Q235A alloys immersed in both the starch concentrations of 300 mg/L and 500 mg/L (Fig. 3).

The electrochemical impedance spectroscopy (EIS) data in this study were fitted using Nova software (Nova Software Inc.) with the equivalent circuit model illustrated in Fig. 3. The circuit components are defined as follows: R_s (solution resistance), electrolyte resistance between the working and reference electrodes. R_p (Polarization resistance), charge transfer resistance at the metal-electrolyte interface. L (Inductive element), associated with surface relaxation or adsorbed intermediate species, Q (constant phase element).

An enhancement in corrosion resistance is observed with an increase in solution resistance R_s , which correlates with a reduction in corrosion current density due to the suppressed charge transfer kinetics at the metal-electrolyte interface.

As per Table 2, the three starch types with the highest R_s values are tapioca, corn, and sweet potato starch, with respective measurements of 0.7056 $\Omega\cdot\text{cm}^{-2}$, 0.6582 $\Omega\cdot\text{cm}^{-2}$, and 0.6267 $\Omega\cdot\text{cm}^{-2}$. Additionally, Table 3 indicates that the starches with the highest R_s levels among the eight varieties tested are pea, wheat, and corn starches, with corresponding values of 0.4634 $\Omega\cdot\text{cm}^{-2}$, 0.4316 $\Omega\cdot\text{cm}^{-2}$ and 0.3815 $\Omega\cdot\text{cm}^{-2}$, respectively. These findings are in agreement with the data illustrated in Fig. 2. In summary, tapioca, corn, and sweet potato starches exhibit the greatest corrosion inhibition efficacy in a solution containing 0.5 mol/L of H₂SO₄ and 300 mg/L of starch [2, 5]. At a starch concentration of 500 mg/L, pea, wheat, and corn starches demonstrate the most pronounced corrosion inhibition effect among the eight starches examined.

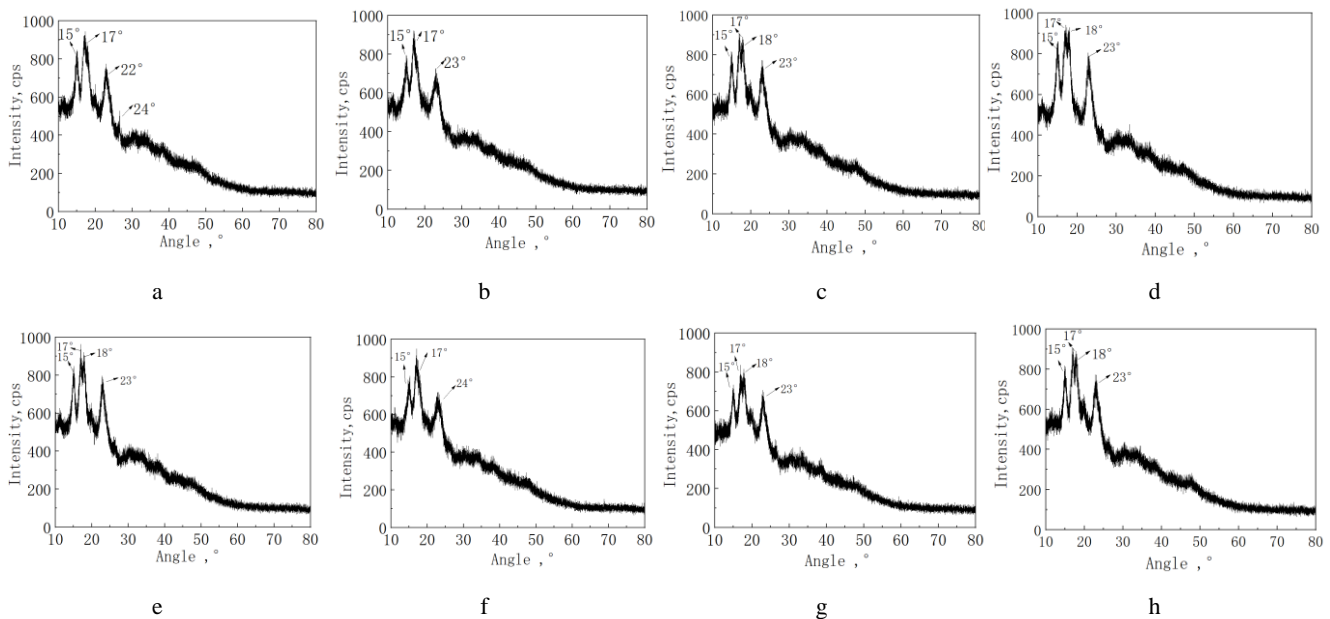


Fig. 1. XRD patterns of eight starches: a–sweet potato starch; b–mung bean starch; c–potato starch; d–cassava starch; e–yam starch; f–pea starch; g–wheat starch; h–corn starch

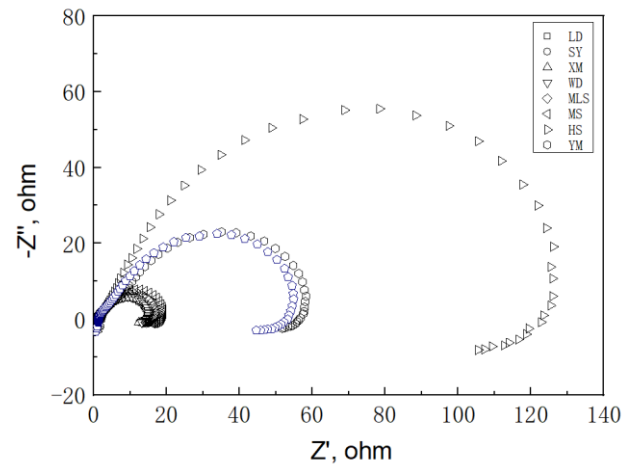
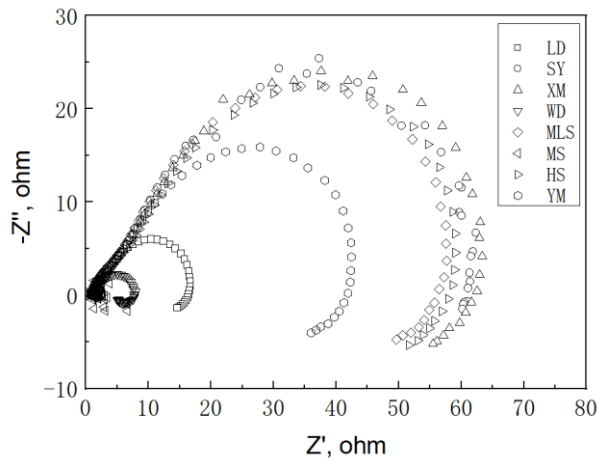


Fig. 2. AC impedance diagram of Q235A steel in 0.5 mol/L H₂SO₄ with starch concentrations: a–300 mg/L; b–500 mg/L

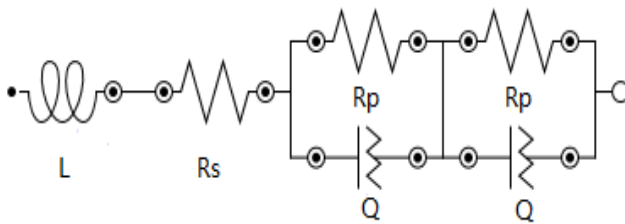


Fig. 3. Equivalent circuit diagram

Fig. 4 presents the microscopic corrosion morphology of the surface of Q235A steel specimens after immersion in a blank 0.5 mol/L H₂SO₄ solution with different types of starch. The metallographic micrographs revealed distinct surface morphological differences between the samples. In the absence of starch additive, the steel surface exhibited a rougher morphology with pronounced corrosion patterns, including visible etching grooves and irregular texture, indicative of severe uniform corrosion. In contrast, the samples treated with starch inhibitors demonstrated a

significantly smoother surface texture, accompanied by a marked reduction in surface irregularities and corrosion-induced features. This contrast underscores the inhibitory role of starch in mitigating surface degradation under acidic conditions.

Fig. 5 displays the Tafel curve for Q235A steel immersed in a 0.5 mol/L H₂SO₄ solution with a starch concentration of 300 mg/L. The results indicate in Table 4 that cassava starch, wheat starch, and potato starch exhibit relatively high corrosion potentials (E_{corr}) at this concentration. Specifically, the corrosion currents for these starches are 26 $\mu\text{A}\cdot\text{cm}^{-2}$, 11 $\mu\text{A}\cdot\text{cm}^{-2}$, and 87 $\mu\text{A}\cdot\text{cm}^{-2}$, respectively, while their polarization resistances (R_p) are 127.54 $\Omega\cdot\text{cm}^{-2}$, 138.2 $\Omega\cdot\text{cm}^{-2}$, and 108.9 $\Omega\cdot\text{cm}^{-2}$, respectively. In contrast, other starches demonstrate negative corrosion potentials relative to these three, accompanied by higher corrosion currents, lower polarization resistances, and consequently, poorer corrosion resistance [6, 7].

Table 2. Corrosion resistance parameters of AC impedance spectra corresponding to the starch concentration of 300 mg/L

Types of starch	$L, \times 10^{-7} \Omega\cdot\text{cm}^{-2}$	$R_s, \Omega\cdot\text{cm}^{-2}$	$R_{p1}, \Omega\cdot\text{cm}^{-2}$	$\text{CPE}_1, \times 10^{-6} \mu\text{F}\cdot\text{cm}^{-2}$	$R_{p2}, \Omega\cdot\text{cm}^{-2}$	$\text{CPE}_2, \times 10^{-6} \mu\text{F}\cdot\text{cm}^{-2}$
LD	12	0.7462	2.685	1961	13.05	2830
SY	63	1.896	55.68	870.3	5.242	528.7
XM	62	1.834	26.46	1617	59.49	1680
WD	36	1.739	17.73	2508	43.32	761.1
MLS	31	0.5101	2.329	783.4	64.35	1684
MS	40	1.801	5.679	1396	10.62	1263
HS	161	5.663	32.66	1166	6.346	2665
YM	54	0.7782	30.01	1142	18.41	908.2

Table 3. Corrosion resistance parameters of AC impedance spectra corresponding to the starch concentration of 500 mg/L

Types of starch	$L, \times 10^{-7} \Omega\cdot\text{cm}^{-2}$	$R_s, \Omega\cdot\text{cm}^{-2}$	$R_{p1}, \Omega\cdot\text{cm}^{-2}$	$\text{CPE}_1, \times 10^{-6} \mu\text{F}\cdot\text{cm}^{-2}$	$R_{p2}, \Omega\cdot\text{cm}^{-2}$	$\text{CPE}_2, \times 10^{-6} \mu\text{F}\cdot\text{cm}^{-2}$
LD	19	0.5531	11.62	1834	2.491	2261
SY	15	0.7961	2.572	2073	11.16	1375
XM	17	0.6214	15.64	3772	13.90	1979
WD	16	0.6389	2.705	1736	15.26	1200
MLS	15	0.7734	2.789	2352	11.31	1558
MS	14	0.8256	2.708	2137	12.79	1156
HS	12	0.5781	2.805	3300	129.1	302.6
YM	11	0.3059	14.02	2138	44.08	447.5

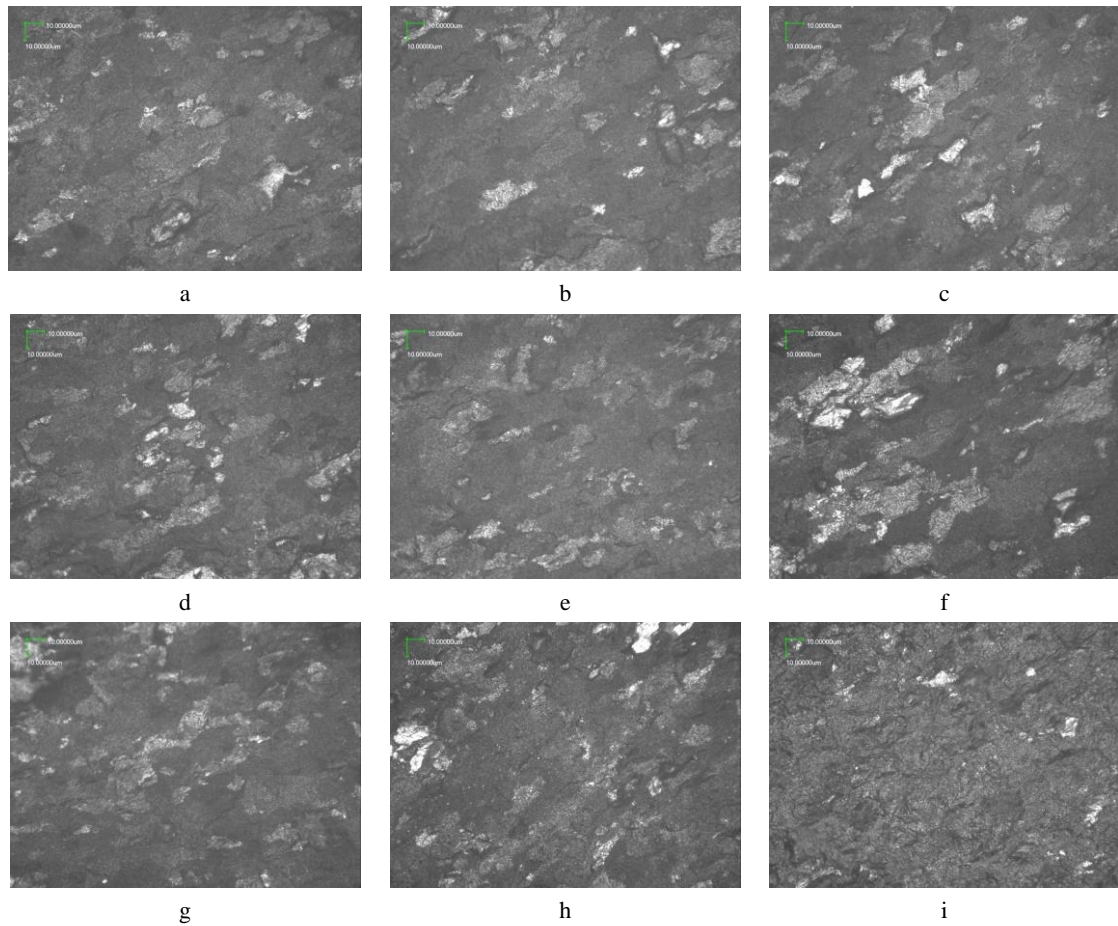


Fig. 4. Metallographic micrographs of Q235A steel after immersion in 0.5 mol/L H_2SO_4 ($\times 100$): a–sweet potato starch; b–mung bean starch; c–potato starch; d–cassava starch; e–yam starch; f–pea starch; g–wheat starch; h–corn starch; i–blank

Therefore, it can be concluded that, under the specified conditions, Q235A steel exhibits superior corrosion resistance in 300 mg/L solutions of cassava starch, wheat starch, and potato starch.

tendency of the steel to corrode. A higher E_{corr} value suggests a lower likelihood of corrosion. In this study, cassava starch, wheat starch, and potato starch were found to have relatively high E_{corr} values, indicating their potential to protect Q235A steel from corrosion. Furthermore, the corrosion current is another critical parameter that reflects the rate of corrosion.

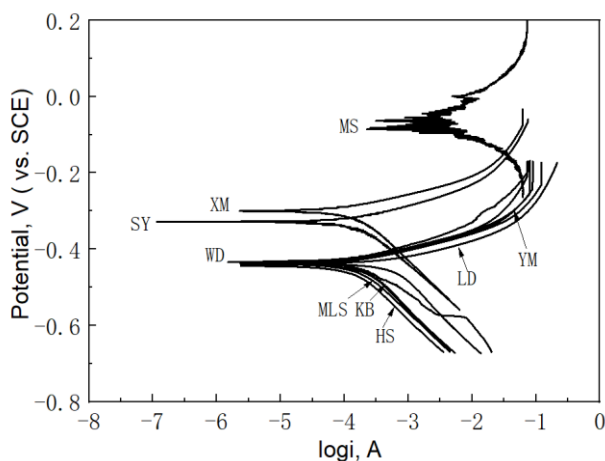


Fig. 5. Tafel diagram of Q235A steel at a starch concentration of 300 mg/L under the condition of 0.5 mol/L H_2SO_4

In more detail, the Tafel curve depicted in Fig. 5 provides valuable insights into the corrosion behavior of Q235A steel in various starch solutions. The corrosion potential (E_{corr}) is a key parameter that indicates the

Table 4. Corrosion resistance parameters of Tafel curve corresponding to 300 mg/L starch

Types of starch	E_{corr} , V	I_{corr} , $\mu A \cdot cm^{-2}$	R_p , $\Omega \cdot cm^{-2}$
LD	-0.4391	125	87.54
SY	-0.3494	87	108.9
XM	-0.3017	11	138.2
WD	-0.4350	34	76.9
MLS	-0.4426	104	100.3
MS	-0.3391	26	127.5
HS	-0.4390	134	78.86
YM	-0.4309	163	62.86

A lower corrosion current signifies a slower corrosion rate [8]. The results showed that the corrosion currents for cassava starch, wheat starch, and potato starch were $26 \mu A \cdot cm^{-2}$, $11 \mu A \cdot cm^{-2}$, and $87 \mu A \cdot cm^{-2}$, respectively, which indicates that the corrosion rate of Q235A steel in these starch solutions is slow. Furthermore, the polarization resistance (R_p) assesses the steel surface's ability to resist

current flow, which correlates with its corrosion resistance.

The efficacy of organic inhibitors in mitigating corrosion can be assessed through the application of the weight loss technique. This method for monitoring corrosion rates is advantageous due to its inherent simplicity and reliability [9]. The bar graph presented in Fig. 6 illustrates the corrosion inhibition rates of various starches on Q235A steel under the specific condition of 0.5 mol/L H₂SO₄ with a starch concentration of 300 mg/L. The results indicate that the corrosion inhibition rates for these starch solutions range from 69 % to 73 %. Notably, tapioca starch, mung bean starch, and wheat starch exhibit higher corrosion inhibition effects, with rates of 72.92 %, 72.89 %, and 72.02 %, respectively. In contrast, the corrosion inhibition rates for potato starch, pea starch, sweet potato starch, and corn starch are relatively similar, falling between 71.95 % and 70.42 %.

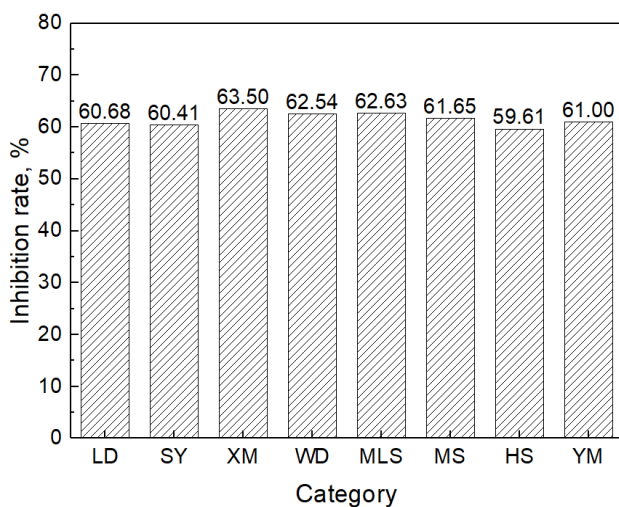


Fig. 6. Histogram of corrosion inhibition rate of Q235A steel soaked in 300 mg/L various starch solutions

These findings suggest that, under the given conditions of 0.5 mol/L H₂SO₄ and 300 mg/L starch concentration, tapioca starch, mung bean starch, and wheat starch achieve superior corrosion inhibition performance on Q235A steel.

4. CONCLUSIONS

The study reveals that various starch solutions, notably those with a concentration of 300 mg/L, exhibit remarkable corrosion inhibition effects on Q235A steel. Particularly, tapioca starch and wheat starch have demonstrated the highest corrosion inhibition efficiencies, achieving 72.92 % and 72.02 %, respectively, under the condition of 0.5 mol/L H₂SO₄.

The electrochemical test methods, including AC impedance spectroscopy, and the Tafel curve, further confirmed that Q235A steel exhibited better corrosion resistance in 300 mg/L starch solution under the same acid concentration. Tapioca starch, wheat starch, and yam starch were found to be particularly effective as corrosion inhibitors.

The crystal structure of starch can be categorized into three main types: A-type, B-type, and C-type. Type A crystals primarily exist in cereal starch and have a relatively compact structure. Type B crystals are primarily

found in the starch of plant tubers and high-amylose crops, with a relatively loose structure. Type C crystals are composed of Type A and Type B crystals, primarily found in the seeds of legume crops and the rhizomes of yam plants. In summary, XRD analysis technology can accurately distinguish and classify the crystal forms of different plant starches, providing an important scientific basis for the research and application of starches.

Based on the promising results obtained in this study, future research can focus on a more detailed investigation of the corrosion inhibition mechanisms of different starches, including their chemical structures and how they interact with the steel surface to prevent corrosion.

Acknowledgments

This work was sponsored by Changzhou Science and Technology Support Project (Social Development) (CE20215036), the Natural Science Foundation of the Jiangsu Higher Education Institutions (No. 17KJA610002), Jiangsu Key Research and Social Development Project (No. BE2017649), Jiangsu Overseas Research & Training Program for University Prominent Young & Middle-aged Teachers and Presidents; Changzhou Institute of technology innovation team project (2020).

REFERENCES

- Zhang, Z., Feng, X.** Synthesis and Evaluation of New Type Plant Extraction Corrosion Inhibitor *Geoenergy Science and Engineering* 245 (2) 2025: pp. 213495. <https://doi.org/10.1016/j.geoen.2024.213495>
- Holla, R.B., Mahesh, R., Manjunath, H.R., Anjanapura, V.R.** Plant Extracts as Green Corrosion Inhibitors for Different Kinds of Steel: A Review *Heliyon* 10 (14) 2024: pp. e33748. <https://doi.org/10.1016/j.heliyon.2024.e33748>
- Chauhan, D.S., Sorour, A.A., Saji, V.S., Quraishi M.A.** Green Corrosion Inhibitors Based on Biomacromolecules and Macrocycles: A review *Sustainable Chemistry and Pharmacy* 36 (10) 2023: pp. 101295. <https://doi.org/10.1016/j.scp.2023.101295>
- Karina Dome E P, Aleksey Bychkov, Lomovsky, O.** Changes in the Crystallinity Degree of Starch Having Different Types of Crystal Structure after Mechanical Pretreatment *Polymers* 16 (12) 2020: pp. 641 <https://doi.org/10.3390/polym12030641>
- Chen, M., Chen, S., Pi, J., Chen, S., Wang, Q., Fu, C.** An investigation of Modified Dialdehyde Starch as A Highly Efficient Green Corrosion Inhibitor for Carbon Steel in 1 M HCl Medium: Synthesis, Experimental and Theoretical Studies *Industrial Crops and Products* 215 2024: pp. 118534. <https://doi.org/10.1016/j.indcrop.2024.118534>
- Tan, B., Liu, Y., Gong, Z., Zhang, X., Chen, J., Guo, L., Xiong, J., Liu, J., Marzouki, R., Li W.** Pyracantha Fortuneana Alcohol Extracts as Biodegradable Corrosion Inhibitors For Copper in H₂SO₄ Media *Journal of Molecular Liquids* 397 2024: pp. 124117. <https://doi.org/10.1016/j.molliq.2024.124117>
- Zhang, Z., Feng, X.** Synthesis and Evaluation of New Type Plant Extraction Corrosion Inhibitor *Geoenergy Science and Engineering* 245 2025: pp. 213495. <https://doi.org/10.1016/j.geoen.2024.213495>

8. **Bello, M., Ochoa, N., Balsamo, V., López-Carrasquero, F., Coll, S., Monsalve, A., González, G.** Modified Cassava Starches as Corrosion Inhibitors of Carbon Steel: An Electrochemical and Morphological Approach *Carbohydrate Polymers* 82 (3) 2010: pp. 561
<https://doi.org/10.1016/j.carbpol.2010.05.019>
9. **KM, S., Praveen, B.M., Devendra, B.K.** A Review on Corrosion Inhibitors: Types, Mechanisms, Electrochemical Analysis, Corrosion Rate and Efficiency of Corrosion Inhibitors on Mild Steel in an Acidic Environment *Results in Surfaces and Interfaces* 16 (8) 2024: pp. 100258
<https://doi.org/10.1016/j.rsurfi.2024.100258>



© Ma et al. 2026 Open Access This article is distributed under the terms of the Creative Commons Attribution 4.0 International License (<http://creativecommons.org/licenses/by/4.0/>), which permits unrestricted use, distribution, and reproduction in any medium, provided you give appropriate credit to the original author(s) and the source, provide a link to the Creative Commons license, and indicate if changes were made.